ME 562 - Assignment 3

Brandon Lampe

March 28, 2015

Abstract

The objective of this assignment was to develop a group of subroutines that systematically calculates and presents results from a defined constitutive model. Additionally, the linear elastic constitutive model was utilized to verify the constitutive equations were correctly implemented. The driver subroutine takes as input prescribed strain increments; therefore, to simulate stress prescribed loading paths with this group of subroutines, certain strain increments required path specific calculations to ensure path constraints were met.

1 Write Driver Program and Verify Strain Paths

A constitutive equation driver program was written to evaluate constitutive models using the Python programming language. The constitutive model for anisotropic elasticity, assuming at least orthotropic symmetry, was developed for use with the driver program. The drive program accepts material parameters, loading path identification, and strain increments. Output from driver program are calculated stresses and strains that result from the prescribed strain increments and loading path type. The driver program relies on seven subroutines written specifically for this effort along with numerous other subroutines written in the python language. The drive program and subroutines the driver program relies on that were written specifically for this effort are listed below along with their respective calling arguments:

1. Matprop(matpropv, elast_parm, visc_parm, elplast_parm) :
   (a) description: calculates material specific elasticity matrix including path specific values
   (b) returns: matpropv
2. Aniso_Elast(matpropv, estrn_incv, estrnv, strsv, path) :
   (a) description: the constitutive equation for anisotropic elasticity, calculates current stress and strain from prescribed strain increments and path type
   (b) returns: estrnv, strsv
3. Constit_Eq(mat_type, leg, matpropv, strn_incm, strnv, estrnv, bstrnv, pstrnv, strsv, path) :
   (a) description: provides a general structure that can be used for calling any constitutive equation, currently calls Aniso_Elast
   (b) returns: strnv, estrnv, bstrnv, pstrnv, strsv
4. Storage(irow, SM, time_step, strsv, strnv, estrnv, bstrnv, pstrnv, histv) :
   (a) description: stores current values of stress and strain; also calculates and stores specific values of stress
   (b) returns: SM, col_namev
5. Plot_Setup(SM, col_namev, out_dir, out_name, sub_plot, path, x1, x2, y1, y2, fmt) :

(a) description: produces plots of data and saves them to a defined location
(b) returns: text stating “Plotting Complete”

6. Term2(irow, limit_deltav) :
   (a) description: determines if the current leg should be terminated based on current value of limit_deltav, provides a binary value used by Driver to determine if the leg should be continued
   (b) returns: cont
7. Limit_Delta(irow, strnv, strsv, p, term_limv, term_type, leg, limit_deltav) :
   (a) description: calculates the difference between the current value and limiting value
   (b) returns: limit_deltav
8. Driver(run_title, n_leg, path_type, term_type, Y1, Y2, Y3, nu12, nu23, nu31, G44, G55, G66, strn_11, strn_22, strn_33, strn_12, mat_type, t_inc, n_nax, inc_max, strs_max, strs_min, strn_max, strn_min, p_max, p_min) :
   (a) description: calls Matprop, Constit_Eq, and Storage, Term2, Limit_Delta
   (b) returns SM, col_namev, irow

Additionally, the driver program relies on SciPy Linear Algebra, NumPy, and MatPlot numerical libraries for general purpose array creation, numerical calculation, and plotting.

1.1 Elasticity Matrix

The subroutine Matrop takes as input up to nine unique elastic parameters, Y, ν, and G; and produces as output the elasticity matrix $[E]_{6x6}$ along with specific elastic matrix elements needed for stress prescribed paths (e.g., for uniaxial stress, plane stress, hydrostatic stress). The following values for elastic parameters were chosen such that the elasticity matrix would have integer-valued components for quick verification, the chosen elastic parameters were:

- $Y_1 = Y_2 = Y_3 = \frac{28}{3}$
- $\nu_{12} = \nu_{23} = \nu_{31} = \frac{1}{6}$
- $G_{44} = G_{55} = G_{66} = \frac{1}{2}$

The resulting components of the elasticity matrix are shown along a description of how the with stress (σ) and strain (e) vectors are defined herein:

$$[E]_{6x6} = \begin{bmatrix} 10 & 2 & 2 & 0 & 0 & 0 \\ 2 & 10 & 2 & 0 & 0 & 0 \\ 2 & 2 & 10 & 0 & 0 & 0 \\ 0 & 0 & 0 & 1 & 0 & 0 \\ 0 & 0 & 0 & 0 & 1 & 0 \\ 0 & 0 & 0 & 0 & 0 & 1 \end{bmatrix}; \quad \{\sigma\}_{6x1} = \begin{Bmatrix} \sigma_{11} \\ \sigma_{22} \\ \sigma_{33} \\ \sigma_{12} \\ \sigma_{23} \\ \sigma_{31} \end{Bmatrix}; \quad \{e\}_{6x1} = \begin{Bmatrix} e_{11} \\ e_{22} \\ e_{33} \\ e_{12} \\ e_{23} \\ e_{31} \end{Bmatrix}$$

Notice the absence of all $\sqrt{2}$ terms that are necessary for typical V-M notation. These terms are not necessary here as no transformations between bases will be performed. Calculations performed by the driver program assume material planes of symmetry are aligned with the normal (’11’, ’22’, and ’33’) directions, as is common in most laboratory tests (e.g., uniaxial stress and triaxial stress). Therefore, a transformation to the Principal basis will not be necessary as the program assumes the normal directions are already aligned with the Principal basis. However, this assumption would not be true for tests that apply a prescribed shear load such as the direct shear test or other forms of torsion tests.

Sign notation for the driver program follows typical mechanics nomenclature, where extension is positive in stress and strain, while compression is both negative in stress and strain. This is opposite of typical geomechanics definitions. Also note that no units were used in the following calculations. Units of calculated stress would be similar to those used in the definitions of the Young’s (Y) and Shear (G) moduli.

1.2 Linear Elastic Uniaxial Strain

The driver program was tested by simulating a uniaxial strain path. Ten strain increments (N_{inc}) were prescribed only in the e_{11} direction, each with a magnitude of 0.01. This resulted in a total strain in the e_{11} direction of 0.10. The linear elastic constitutive equation, used for calculations in this analysis, is:

$$\{\sigma\}_{6x1} = [E]_{6x6}\{e\}_{6x1}$$

Analytical solutions to the components of stress for the defined orthotropic material were solved and were used to verify driver program results. The calculated results of these components are shown below:

- Final $\Delta\sigma_{11} = N_{inc}(E_{11}\Delta e_{11} + E_{12}\Delta e_{22} + E_{13}\Delta e_{33}) = 10 * (10 * 0.01 + 2 * 0 + 2 * 0) = 1.0$
- Final $\Delta\sigma_{22} = \Delta\sigma_{33} = N_{inc}(E_{21}\Delta e_{11} + E_{22}\Delta e_{22} + E_{23}\Delta e_{33}) = 10 * (2 * 0.01 + 10 * 0 + 2 * 0) = 0.2$
- Final $\Delta\sigma_{12} = \Delta\sigma_{23} = \Delta\sigma_{31} = N_{inc}(E_{44}\Delta e_{12} + E_{45}\Delta e_{23} + E_{46}\Delta e_{31}) = 10 * (1 * 0 + 0 * 0 + 0 * 0) = 0$

Graphical results from the driver program for this analysis are shown in Figures 1 and 2. The first figure shows the prescribed strains e_{11} and e_{22} with respect to calculated stress σ_{11}, and the second figure shows stresses σ_{22} and σ_{12} with respect to prescribed strain e_{11}. Final values of stress and strain agree with both the intended prescribed values and the final analytical solutions shown above:

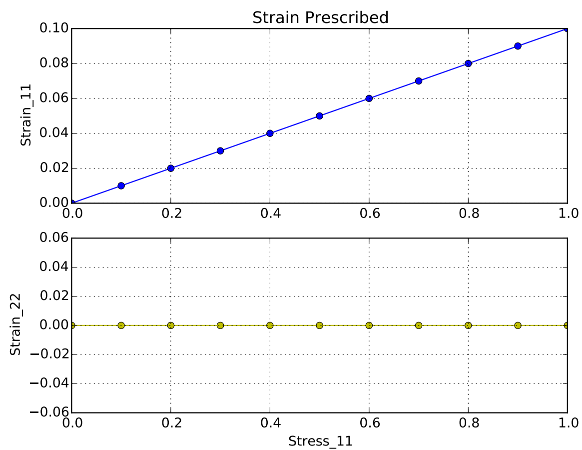

Figure 1: Strains in the '11' and '22' directions versus stress in the '11' direction for a uniaxial strain analysis.

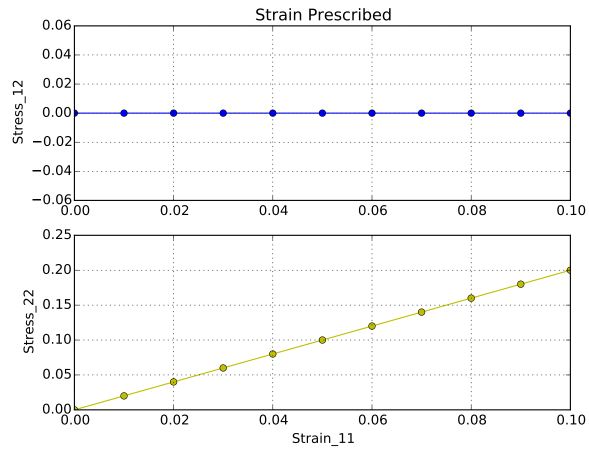

Figure 2: Stresses in the '12' and '22' directions versus strain in the '11' direction for a uniaxial strain analysis.

1.3 Linear Elastic Plane Strain

A plane strain path was simulated with the e_{11}, e_{22}, and e_{12} strains only; again, ten strain increments were prescribed. Each strain increment had a magnitude of 0.01, which resulted in total strains of 0.12 for e_{11} and e_{22}, and e_{12} and zero strain in all other directions. Analytical solutions to the calculated stresses are shown below and were used to verify the correct numerical results from the driver program.

- Final $\Delta\sigma_{11} = N_{inc} * (E_{11}\Delta e_{11} + E_{12}\Delta e_{22} + E_{13}\Delta e_{33}) = 10 * (10 * 0.01 + 2 * 0.01 + 2 * 0) = 1.2$
- Final $\Delta\sigma_{22} = N_{inc} * (E_{21}\Delta e_{11} + E_{22}\Delta e_{22} + E_{23}\Delta e_{33}) = 10 * (2 * 0.01 + 10 * 0.01 + 2 * 0) = 1.2$
- Final $\Delta\sigma_{33} = N_{inc} * (E_{31}\Delta e_{11} + E_{32}\Delta e_{22} + E_{33}\Delta e_{33}) = 10 * (2 * 0.01 + 2 * 0.01 + 10 * 0) = 0.4$
- Final $\Delta\sigma_{12} = \Delta\sigma_{23} = N_{inc} * (E_{44}\Delta e_{12} + E_{45}\Delta e_{23} + E_{46}\Delta e_{31}) = 10 * (1 * 0.01 + 0 * 0.01 + 0 * 0) = 0.1$
- Final $\Delta\sigma_{31} = N_{inc} * (E_{44}\Delta e_{12} + E_{45}\Delta e_{23} + E_{46}\Delta e_{31}) = 10 * (0 * 0.01 + 0 * 0.01 + 1 * 0) = 0$

Graphical results of select stress and strain values are shown below in Figures 3 and 4. Figure 3 shows the calculated total value of $\Delta\sigma_{11}$ agrees with results from the driver program and verifies the prescribed strain increments Δe_{11} and Δe_{12} were correctly implemented. Figure 4 presents the calculated values of stress in the '33' and '12' directions against strain in the '11' direction, again final values in these figures agree with the hand calculations shown above.

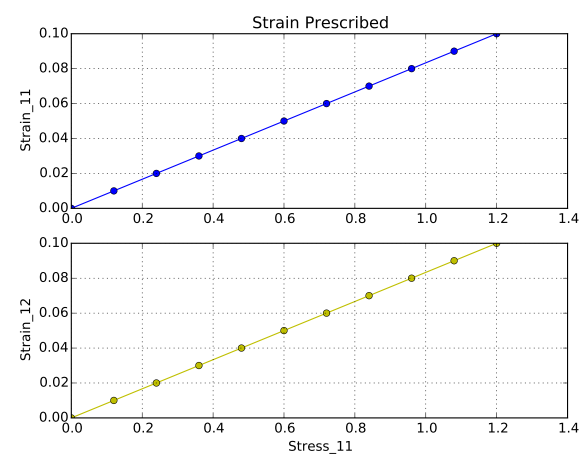

Figure 3: Strains in the '11' and '12' directions versus stress in the '11' direction for a plane strain analysis.

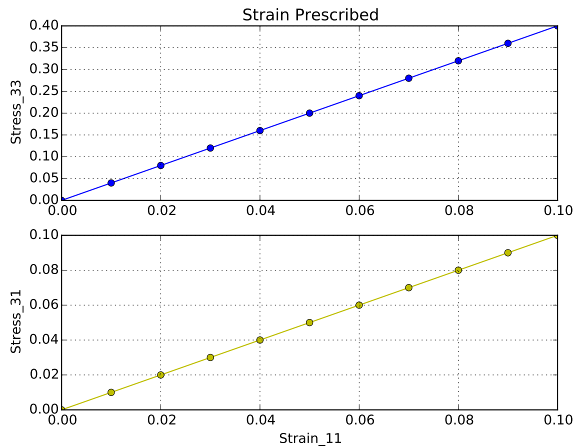

Figure 4: Stresses in the '33' and '12' directions versus strain in the '11' direction for a plane strain analysis.

2 Show that Driver Program Can Model Cyclic Paths

The driver program is able to perform cyclic loading by defining multiple legs in a prescribed loading path, each leg having a different value of stress increment (e.g., $+\Delta e_{11}$ then $-\Delta e_{11}$). Each leg of the path may also be terminated by a different criterion (e.g., . The program appears to operate correctly on all accounts as long as the same strain increments are prescribed for each leg; however, when the strain increments vary in size the termination criteria may be "over stepped" if the criteria is reached in the middle of a strain increment. The magnitude of this "over step" may be minimized by prescribing suitably small strain increments.

2.1 Cycle in Uniaxial Strain

Two cycles in uniaxial strain were performed, legs of the cycle were terminated by maximum and minimum values of σ_{11}. The maximum and minimum values of σ_{11} were 0.8 and -0.6, respectively, and the strain increment size was held constant at 0.01 for each of the 68 prescribed increments applied over the five different legs. Figure 5 depicts the results of the modeled cycle. Computed stresses were easily verified using the equation for uniaxial stress increment provided in Section 1.2.

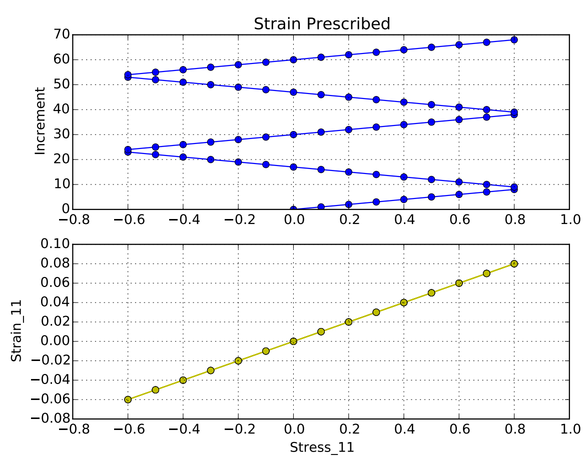

Figure 5: e_{11} and increment number versus σ_{11} for two cycles in uniaxial strain.

2.2 Cycle in $e_{11} - e_{12}$ Strain Space

A rectangular cycle in the $e_{11} - e_{12}$ strain space was was completed. The rectangular cycle consisted of four legs, each leg was terminated after 10 strain increments, which resulted in a total of 40 increments. Figure 6 shows both the $\sigma_{11} - \sigma_{12}$ and $e_{11} - e_{12}$ spaces, which are both rectangular in shape. Again, numerical values from the driver program agree with hand calculations made use equations provided in Section 1. Figures 7 and 8 show strain and increment number versus stress for both the '11' and '12' directions. These figures provide evidence that the prescribed cycles are correctly being executed.

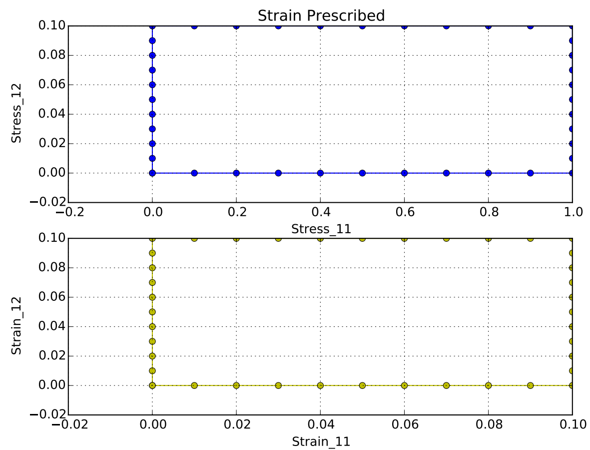

Figure 6: Stress and strain paths during the rectangular cycle.

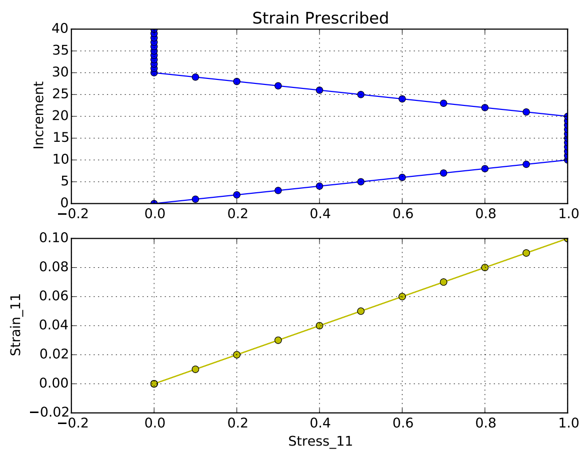

Figure 7: e_{11} and increment number versus σ_{11} during the rectangular cycle.

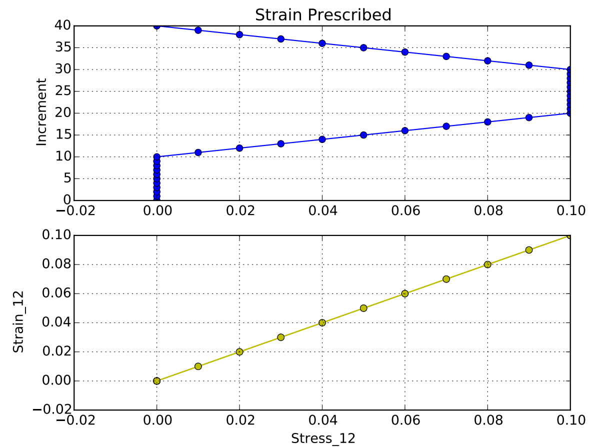

Figure 8: e_{12} and increment number versus σ_{12} during the rectangular cycle.

3 Apply Constitutive Equation Constraints for Stress Defined Paths

The driver program was designed to calculate stress increments resulting from prescribed strain increments; however, there are many laboratory tests performed that prescribe a specific stress state.

3.1 Uniaxial Stress

Uniaxial stress implies that stress is applied only along one axis (σ_{11}) and the other components of stress are zero. To allow for this path in the driver program, uniaxial specific components of the elasticity matrix must be defined such that the following set of equations are satisfied:

$$\begin{Bmatrix} \Delta\sigma_{11} \\ 0 \\ 0 \end{Bmatrix} = \begin{bmatrix} E_{11} & E_{12} & E_{13} \\ E_{21}^{UX} & E_{22} & E_{23} \\ E_{31}^{UX} & E_{32} & E_{33} \end{bmatrix} = \begin{Bmatrix} \Delta e_{11} \\ \Delta e_{22} \\ \Delta e_{33} \end{Bmatrix}$$

Where E_{21}^{UX} and E_{31}^{UX} are specific for a uniaxial stress path, with stress in the '11' direction, and allow for the appropriate values of Δe_{22} and Δe_{33} to be calculated such that the remaining stress increments, $\Delta\sigma_{22}$ and $\Delta\sigma_{33}$, equal zero. Verification of the correct E_{21}^{UX} and E_{31}^{UX} values was completed by simulating a load cycle with prescribed stress limits of 1.0 and -1.0 for the maximum and minimum values, along with Δe_{11} of 0.01 and -0.01, respectively (Figure 9). The uniaxial condition requires σ_{22} and σ_{33} to equal zero, this result has been verified and is shown in Figure 10. Δe_{11} and Δe_{22} were overridden such that the uniaxial stress condition would be satisfied, the resulting strains are shown in Figure 11. The result of all other strain increment values were zero

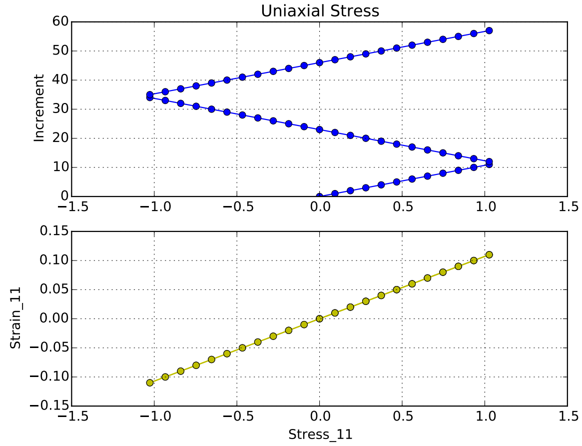

Figure 9: σ_{11} and increment number versus e_{11} for one cycle of uniaxial stress.

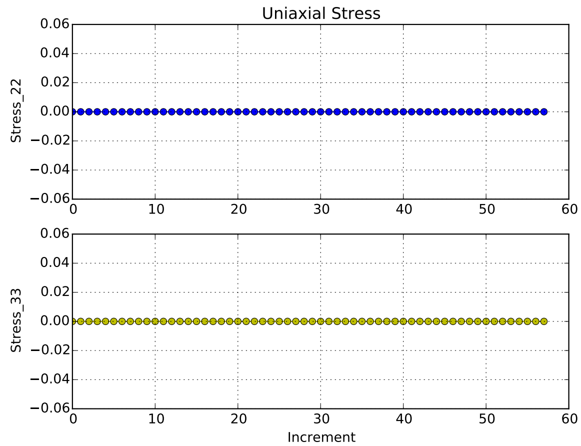

Figure 10: σ_{22} and σ_{33} versus increment number for one cycle of uniaxial stress.

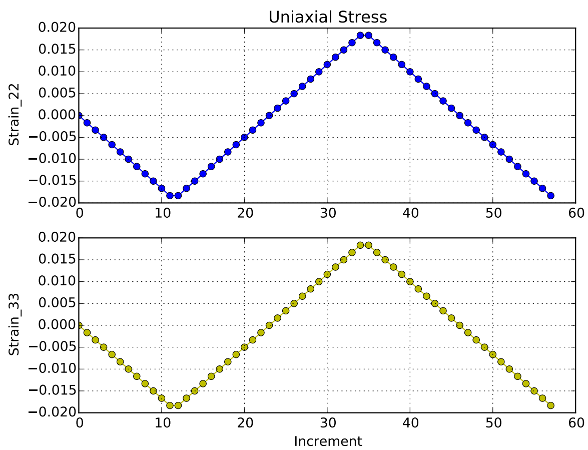

Figure 11: e_{11} and e_{22} versus increment number for one cycle of uniaxial stress.

3.2 Hydrostatic Stress

A similar method of modifying components of the elasticity matrix was used for calculating a hydrostatic stress path. Again, E_{21} and E_{31} were replaced with hydrostatic stress path specific values of E_{21}^H and E_{31}^H. For hydrostatic stress, values of Δe_{22} and Δe_{33} were then calculated to constrain the values a normal stress such that $\sigma_{11} = \sigma_{22} = \sigma_{33}$ and all other values of stress equal zero. Verification was again completed by prescribing strain increments with values of 0.01 and -0.01 and each leg would terminate at a defined stress limit of 1.0 and -1.0, respectively. The results of the verification are shown below in terms of a q_1 versus mean stress p and increment number versus p(Figure 12). Additionally, to verify that stress was indeed hydrostatic, σ_{11} and σ_{22} versus increment number are also provided (Figure 13).

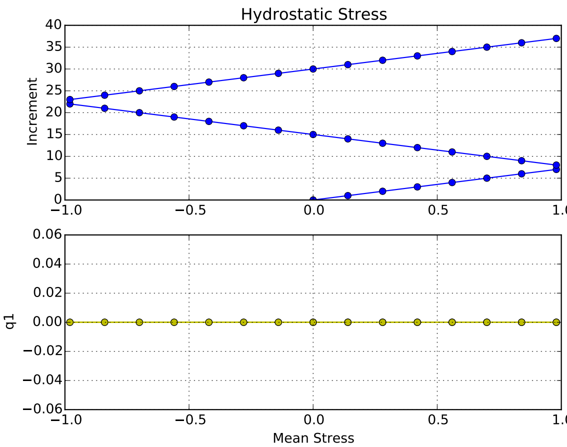

Figure 12: Increment number and q_1 versus mean stress for a hydrostatic stress cycle.

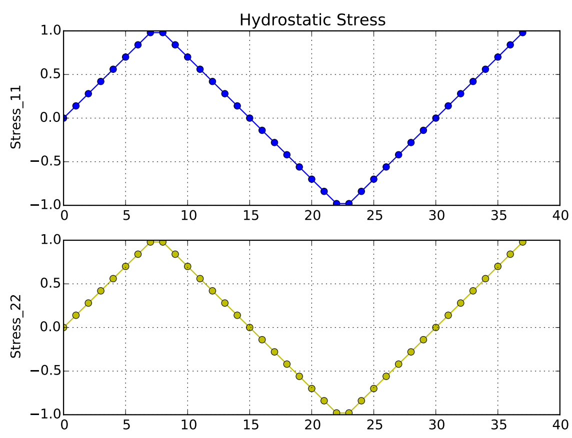

Figure 13: σ_{11} and σ_{22} versus increment number for a hydrostatic stress cycle.

3.3 Triaxial Compression

Triaxial compression was simulated using two legs. The first leg applied a hydrostatic compressive stress to a prescribed value of p_0, and the second leg increased compressive stress σ_{11} while maintaining $\sigma_{22} = \sigma_{33} = p_0$. The relationship for the final state of stress is shown below :

$$\sigma_{11} < \sigma_{22} = \sigma_{33} = p_0$$

Initially, stress was hydrostatically decreased (compression) with prescribed strain increments of $\Delta e_{11} = -0.001$ until a minimum mean stress was reached ($p_0 = -0.5$). The second leg was then initiated, $\Delta e_{11} = -0.005$ while the triaxial condition $\sigma_{22} = \sigma_{33} = p_0$ was maintained by calculating the needed values of $\Delta e_{22} = \Delta e_{33}$. The second leg was terminated when $\sigma_{11} = -1.0$. Figure 14 below shows values of q and σ_{11} versus mean stress (p), where:

$$q = q_1 + q_2 = \text{Mises Stress}$$

$$q_1 = \frac{\sqrt{3}}{2}(\sigma_2^{dev} - \sigma_1^{dev})$$

$$q_2 = -\frac{3}{2}(\sigma_1^{dev} + \sigma_2^{dev})$$

$$p = (\sigma_1 + \sigma_2 + \sigma_3)/3 = \text{Mean Stress}$$

Values above with one subscript represent a principal stress value (e.g., σ_1,σ_2, and σ_3) and the superscripts *dev* indicate these are principal components of the deviator stress matrix.

Figure 15 shows how σ_{22} and σ_{33} varied with respect to σ_{11} during both legs of the test. Figure 16 shows the required values of e_{22} and e_{33} for the condition $\sigma_{22} = \sigma_{33} = p_0$ to be maintained.

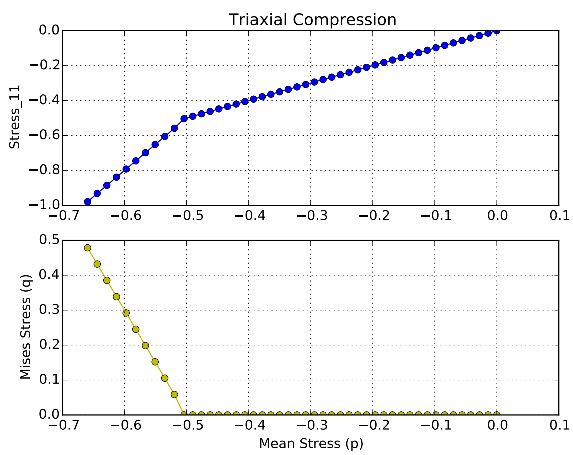

Figure 14: q and σ_{11} versus mean stress (p) for the hydrostatic and triaxial compression legs.

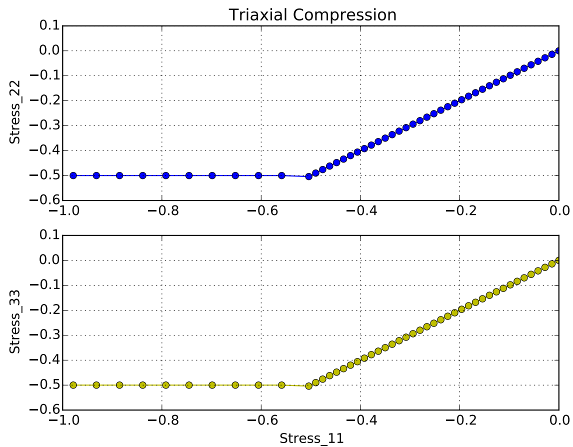

Figure 15: σ_{22} and σ_{33} versus σ_{11} for the hydrostatic and triaxial compression legs.

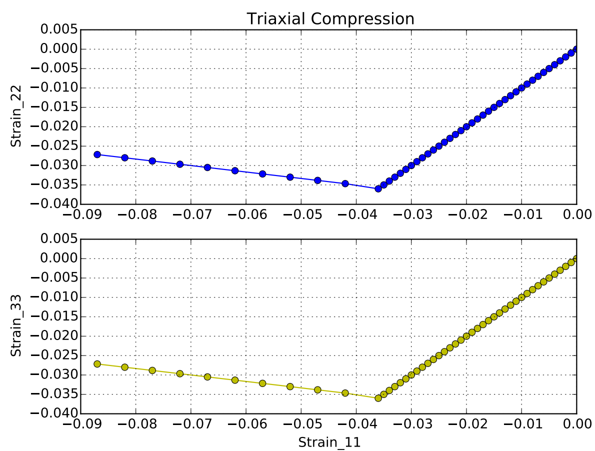

Figure 16: e_{22} and e_{33} versus e_{11} for the hydrostatic and triaxial compression legs.

3.4 Triaxial Extension

Triaxial extension was also simulated using two legs, the first was hydrostatic compression and the second was triaxial extension. The triaxial extension stress path was defined such that:

$$\sigma_{11} > \sigma_{22} = \sigma_{33} = p_0$$

Strain increments during hydrostatic compression were prescribed as $\Delta e_{11} = -0.001$. Triaxial extension was initiated during the second leg by prescribing strain increments of $\Delta e_{11} = 0.005$ (extension) and calculating the needed values of $\Delta e_{22} = \Delta e_{33}$ in order to maintain $\sigma_{22} = \sigma_{33} = p_0$. The first leg was terminated by a minimum $p_0 = -0.5$, and the second leg was terminated by maximum stress $\sigma_{11} = -0.15$. Figure 17 depicts stress in the Rendulic plane $(q - p)$ and σ_{11} versus $p$while Figure 18 illustrates stresses during both the hydrostatic and triaxial extension legs.Figure 19 shows the calculated values of e_{11} and e_{22} needed to maintain the triaxial extension constraint.

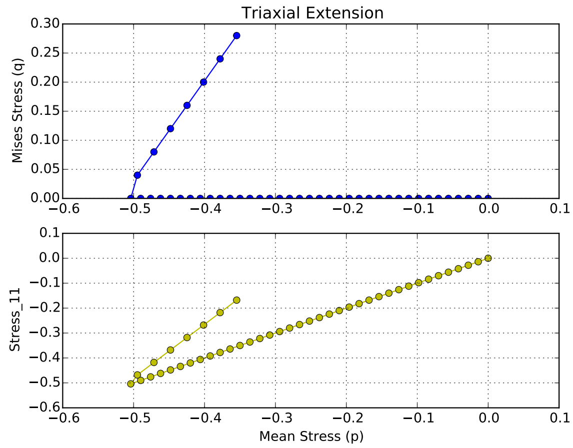

Figure 17: q and σ_{11} versus mean stress (p) for the hydrostatic and triaxial extension legs.

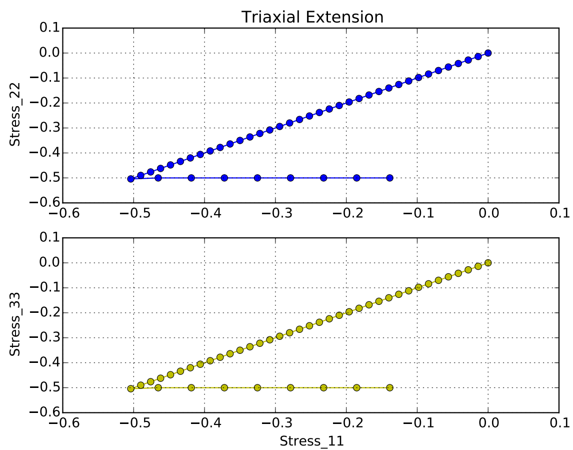

Figure 18: σ_{22} and σ_{33} versus σ_{11} for the hydrostatic and triaxial extension legs.

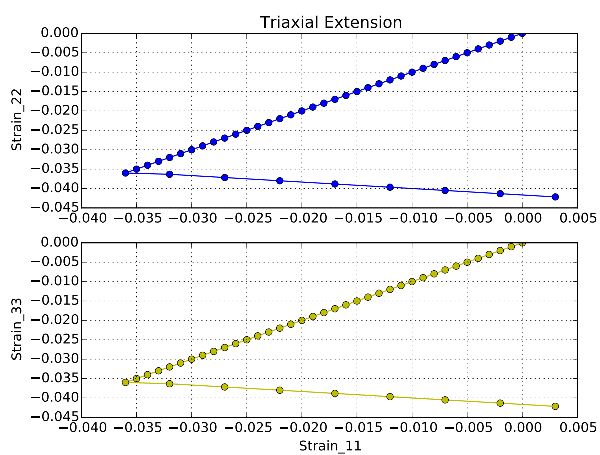

Figure 19: e_{22} and e_{33} versus e_{11} for the hydrostatic and triaxial extension legs.